The Meteoritical Society

Meteoritics & Planetary Science 46, Nr 6, 875–889 (2011)
doi: 10.1111/j.1945-5100.2011.01199.x

The complex impact structure Serra da Cangalha, Tocantins State, Brazil

Thomas KENKMANN[1*], Marcos A. R. VASCONCELOS[2,3], Alvaro P. CRÓSTA[2], and Wolf U. REIMOLD[3]

[1]Institut für Geowissenschaften—Geologie, Albert-Ludwigs-Universität Freiburg, Albertstrsse 23-b, 79104 Freiburg, Germany
[2]Institute of Geosciences, University of Campinas, R. Pandiá Calógeras 51, 13083-970, Campinas, São Paulo, Brazil
[3]Museum für Naturkunde, Leibniz-Institut an der Humboldt-Universität zu Berlin, Invalidenstraße 43, 10115 Berlin, Germany
[*]Corresponding author. E-mail: thomas.kenkmann@geologie.uni-freiburg.de

(Received 16 September 2010; revision accepted 18 February 2011)

Abstract–Serra da Cangalha is a complex impact structure with a crater diameter of 13,700 m and a central uplift diameter of 5800 m. New findings of shatter cones, planar fractures, feather features, and possible planar deformation features are presented. Several ring-like features that are visible on remote sensing imagery are caused by selective erosion of tilted strata. The target at Serra da Cangalha is composed of Devonian to Permian sedimentary rocks, mainly sandstones that are interlayered with siltstone and claystones. NNE–SSW and WNW–ESE-striking joint sets were present prior to the impact and also overprinted the structure after its formation. As preferred zones of weakness, these joint sets partly controlled the shape of the outer perimeter of the structure and, in particular, affected the deformation within the central uplift. Joints in radial orientation to the impact center did not undergo a change in orientation during tilting of strata when the central uplift was formed. These planes were used as major displacement zones. The asymmetry of the central uplift, with preferred overturning of strata in the northern to western sector, may suggest a moderately oblique impact from a southerly direction. Buckle folding of tilted strata, as well as strata overturning, indicates that the central uplift became gravitationally unstable at the end of crater formation.

INTRODUCTION

Serra da Cangalha (centered at 8°05′ S/46°52′ W) is a complex impact structure at the border between Tocantins and Maranhao states of Brazil. Dietz and French (1973) were the first who drew attention to the structure, but they were not able to confirm its impact origin. Further work on Serra da Cangalha was carried out by McHone (1979), Santos and McHone (1979), McHone (1986), and Crósta (1987). However, published evidence for impact origin in the form of shatter cones and bona fide shock deformation remained scarce (Crósta 2004; Reimold et al. 2006).

The structure is located within the intracratonic Parnaíba basin filled with Upper Silurian to Cretaceous sedimentary rocks (Crósta 1982, 1987). Based on stratigraphic considerations, the age of the structure has been delimited to <250 Ma, the age of the youngest strata affected by the formation of the structure. The wider region of the sedimentary basin around Serra da Cangalha appears undeformed, with flat-lying strata and a morphology dominated by table mountains. Recently, several geophysical studies have been carried out at Serra da Cangalha (Adepelumi et al. 2004, 2005; Abraham et al. 2004; Vasconcelos et al. 2010a), which involved gravity and aeromagnetic analysis, as well as resistivity and magnetotelluric modeling. According to the interpretation of Adepelumi et al. (2005), the crystalline basement in the region of Serra da Cangalha occurs at a depth of 1.1–1.5 km. However, Vasconcelos et al. (2010a), based on regional aeromagnetic data, interpreted the depth to basement underneath the structure as 2400 m, pointing out that this estimation is in accordance with data from an oil exploration borehole located 70 km north of Serra da Cangalha. Serra da Cangalha exhibits a 10 nT magnetic high that is offset

from the center (Vasconcelos et al. 2010a) and a semicircular gravity low shifted 7 km to the north of the center. Its relation to the structure is obscure. Three boreholes approximately 200 m deep (GT-01-GO; GT-02-GO; GT-03-GO) were drilled into the central crater depression in the early 1970s by the Brazilian Department of Mineral Production in the framework of a mineral exploration campaign.

Remote sensing studies by Almeida-Filho et al. (2005) using ASTER (Advanced Spaceborne Thermal Emission) data and by Reimold et al. (2006) based on Shuttle Radar Topographic Mission (SRTM) and Landsat Thematic Mapper data have been carried out in recent years and yielded detailed topographic information emphasizing several ring-like features. Most prominent is a central ring structure of approximately 3 km diameter. This inner ring was revealed to comprise an annular ring of 250–300 m high hills of intensely deformed sedimentary rocks enclosing a near-circular depression. Reimold et al. (2006) also reported less prominent outer ring structures at Serra da Cangalha. The outer edge of the structure was defined by a series of flattish plateaus. This remote sensing analysis stimulated our field survey to unravel the nature of the circular features: are the observed rings comparable to circular features of planetary craters, or are they simply the result of selective erosion of a dome-like uplift?

This work is part of a multidisciplinary investigation of Serra da Cangalha and environs and involves (1) detailed structural mapping of the entire structure with a focus on the central uplift area, (2) statistical analysis of the structural inventory aimed at elucidating the kinematic history of the event and constraining the influence of target heterogeneities and impact trajectory on crater formation, (3) documentation of impact deformation at microscales to macroscales, and (4) the confirmation of the impact origin of the structure. First results of this study have been presented in abstract form by Kenkmann et al. (2010a) and Vasconcelos et al. (2010b). Different aspects of the consortium study, such as more detailed shock petrography and the geophysical results, are prepared separately from the present report.

METHODS

In the course of the field campaign, 472 GPS referenced data points were recorded, with notation of lithology, bedding plane orientation, and structure (Fig. 1). Dense vegetation and soil/sand cover limited access to exposure in the moat between the collar around the central elevated area and the crater rim, and in the inner depression within the central uplift structure. Samples were taken from every lithology. Standard polished thin sections were manufactured for inspection of the petrography and microstructure using a polarizing microscope. A universal stage was used to index the crystallographic orientation of planar microstructures. The collected field data consist of dip azimuth and dip angle values, along with latitude and longitude of bedding planes, as well as structural data. The declination correction is −19° W. Errors on GPS coordinates given in the GPS recordings are usually in the order of 6 m; on strata orientations and other planar structures (e.g., faults) the error is 5°. For mapping purposes, we used georeferenced CBERS-2B/HRC (China-Brazil Earth Resources Satellite/High Resolution Camera) (2.7 m resolution) and WorldView-1 (0.5 m resolution) satellite images, as well as ASTER data. Geologic surveying and mapping were performed using the ARCGIS 9.31 software package by ESRI. Lineaments and faults were constructed as polylines. The coordinates of start-point, end-point, and midpoint of each polyline were recorded to determine the mean distance of the lines from the center of the structure and to calculate the strike of mapped lineaments. Geographic coordinates of data points, faults, and lineaments were then translated into a radial framework with the point of origin placed into the crater center. The crater center is defined as the midpoint of a circle fitted to the collar of the central uplift. We calculated the azimuth for all data with respect to the crater center. The azimuthal position thus gives an angular value in relation to the crater center: e.g., a data point directly north of the center has a value of 0°, one to the east has a value of 90°, etc.

Further transformations are necessary to specify the degree of radial symmetry within the crater and to express the orientation of linear features by means of their concentric or radial component. The strike of rock layers, lineations, and faults was compared with the tangential orientation or "concentric strike" of a circle with a point of origin in the crater center. The difference between the two produced an angular value for each measurement, which, depending on the orientation of strike, is either positive or negative (Poelchau and Kenkmann 2008). The angle is positive if the measured strike deviates clockwise from the tangential position, and negative if the measured strike deviates counterclockwise from the tangential position. These values are referred to as the *angular deviation from concentric strike* or, in short, the *concentric deviation* (Poelchau and Kenkmann 2008). To calculate the concentric deviation, it is first assumed that the maximum amount of horizontal rotation experienced by the strike during crater excavation was less than 90°, as observed in the field. For data conversion, the precise latitude and longitude of the crater center and of the measurement point are necessary. The concentric deviation is plotted against the azimuthal position or the

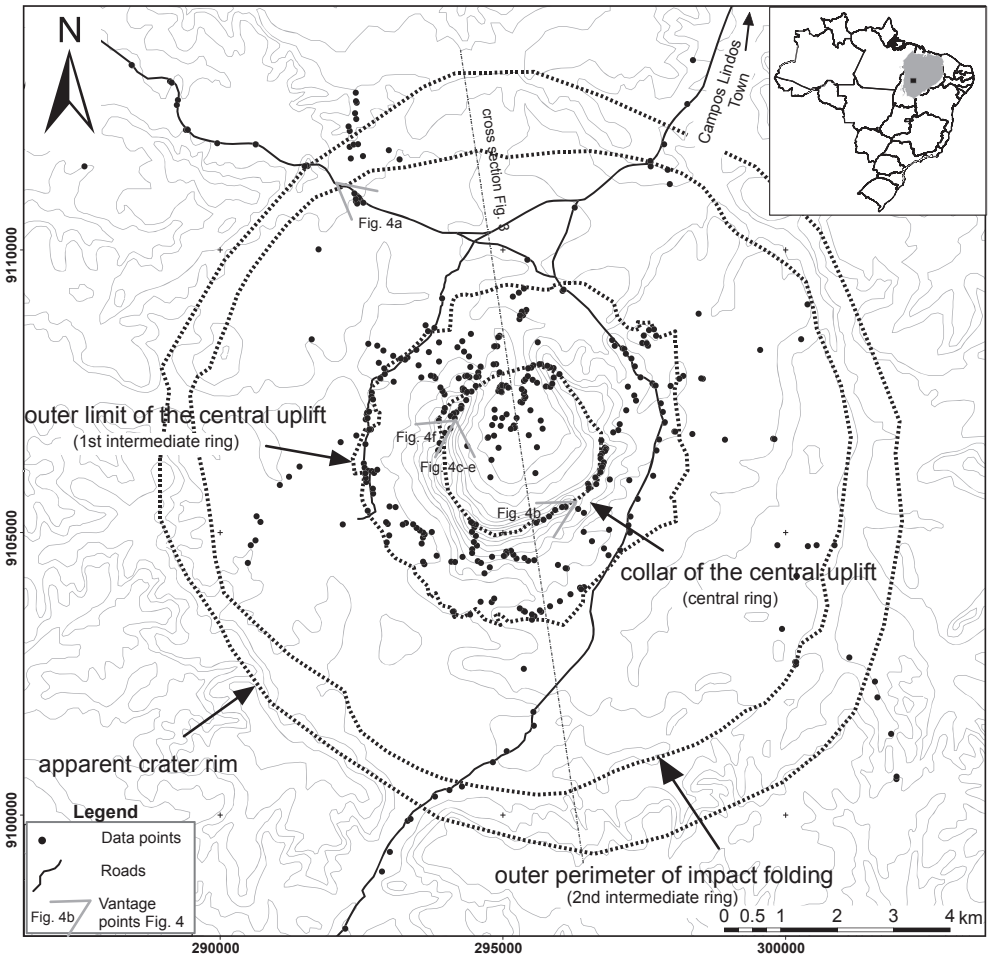

Fig. 1. Topographic map of the Serra da Cangalha impact structure. Stippled lines represent major circular features observed in satellite imagery and in the field. For comparison, the terminology of ring features used by Reimold et al. (2006) has been added in smaller font in brackets. Dots are locations (data points), where data were recorded in this study. Inset shows the location of the structure in Tocantins province of north-central Brazil (UTM coordinates).

radial distance from the crater center. A detailed mathematical description of the transformation and the determination of the value of "concentric deviation" is given in Poelchau and Kenkmann (2008).

RESULTS

Stratigraphy

Lithostratigraphic detail was given in Crósta (1982, 1987) and Vasconcelos et al. (2010b). Detailed stratigraphic information for the Parnaíba basin sequence is found in Góes and Feijó (1994). Herein, we briefly review the stratigraphic units as they were mapped in this study. The lowermost stratigraphic unit exposed at Serra da Cangalha is the Longá Fm., belonging to the Canindé Group of Devonian age. This formation is dominated by dark shales and siltstones, and is locally exposed in the center of the structure (Figs. 2 and 3), where it was drilled by the Brazilian Department of Mineral Production in the 1970s. Its high susceptibility to erosion is responsible for the lower elevation of this central area and for its lack of outcrops. The tectonic situation in the center of the structure is very complex, so that the lithostratigraphic context has been essentially lost. The occurrence of Longá Fm. always correlates with morphological lows.

Stratigraphically above the Longá Fm. occurs the Poti Fm., a prominent mountain builder with high resistivity to erosion (Figs. 4B–F). The Poti Fm. comprises massive, decameter-thick quartzitic beds of Carboniferous sandstones and builds the prominent collar of the central uplift structure (Figs. 2 and 3). A few incompetent beds exist that subdivide the formation and allow flexural slip folding (Figs. 4B, 4D, and 4F). A detailed stratigraphic succession within the Poti Fm. could not be derived due to the complex tectonic situation.

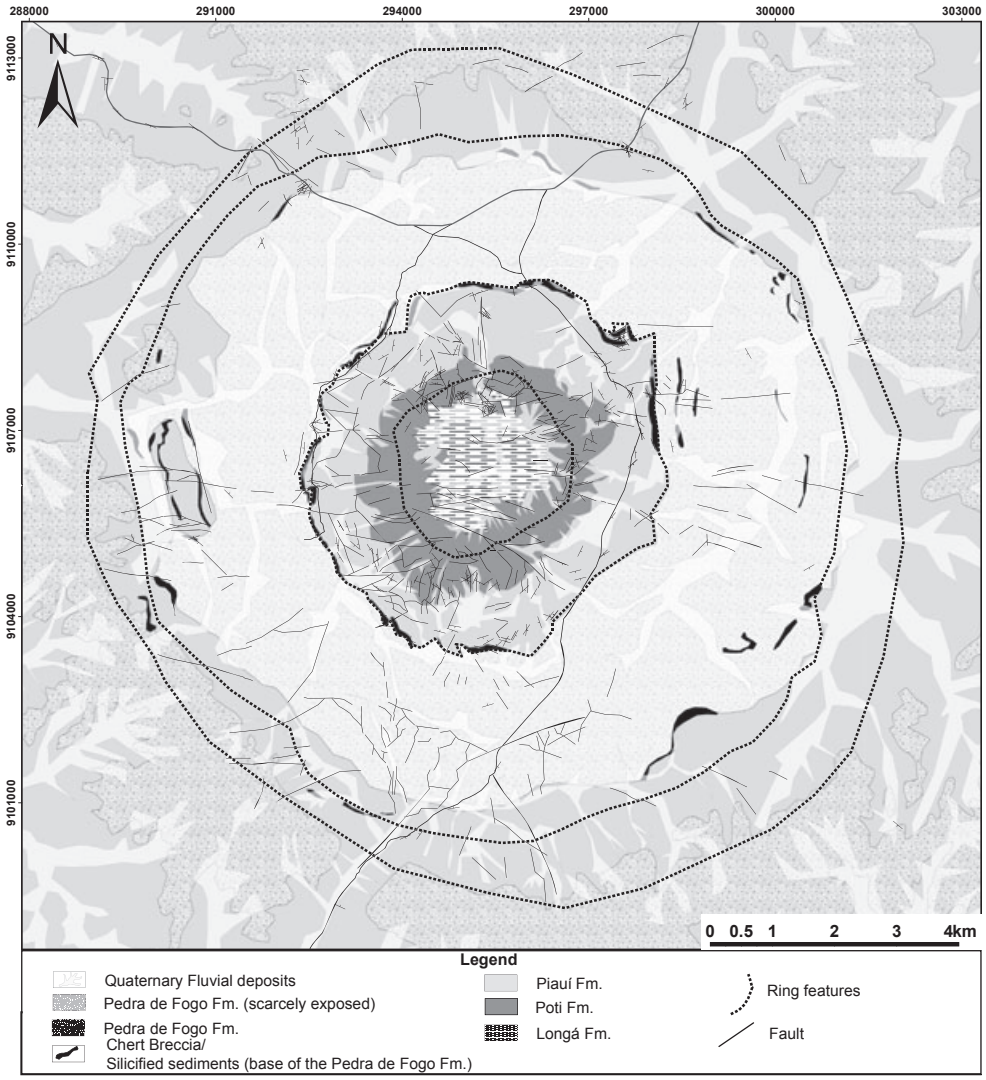

Fig. 2. Geological map of the Serra da Cangalha impact structure compiled from data collected during our field survey and using remote sensing analysis. A more detailed map of the central uplift area is given in Fig. 7. The oldest beds crop out in the center and are surrounded by successively younger strata. Strata of the syncline around the central uplift are poorly exposed. Mapping of this annulus therefore relies heavily on the interpretation of remote sensing data.

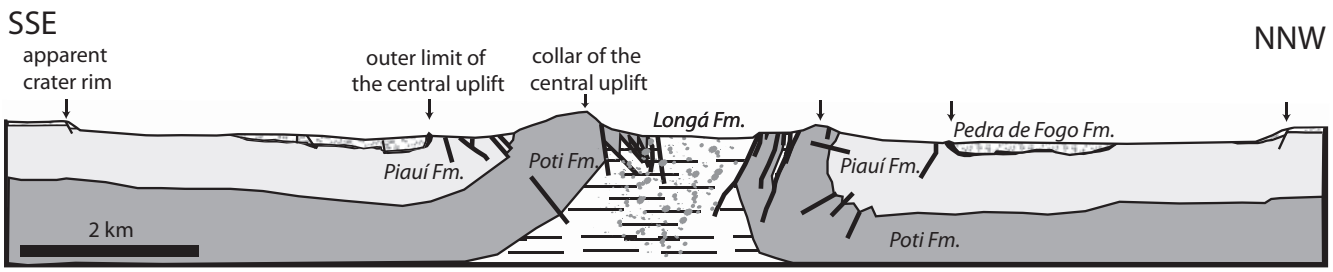

Fig. 3. Schematic geological cross section through the Serra da Cangalha structure along a NNW–SSE (170°) trend. Note that the northern part of the central uplift is characterized by overturned strata, whereas the southern part is not. Vertical exaggeration is approximately 2×.

The Piauí Fm. (Figs. 2 and 3), stratigraphically above the Poti Fm., forms the periphery of the central uplift and shows a distinct layering. It is composed of intercalated sandstone-siltstone-claystone beds (Fig. 4A). Sandstones display cross stratification. As the proportion of incompetent beds is greater in the Piauí Fm. than in

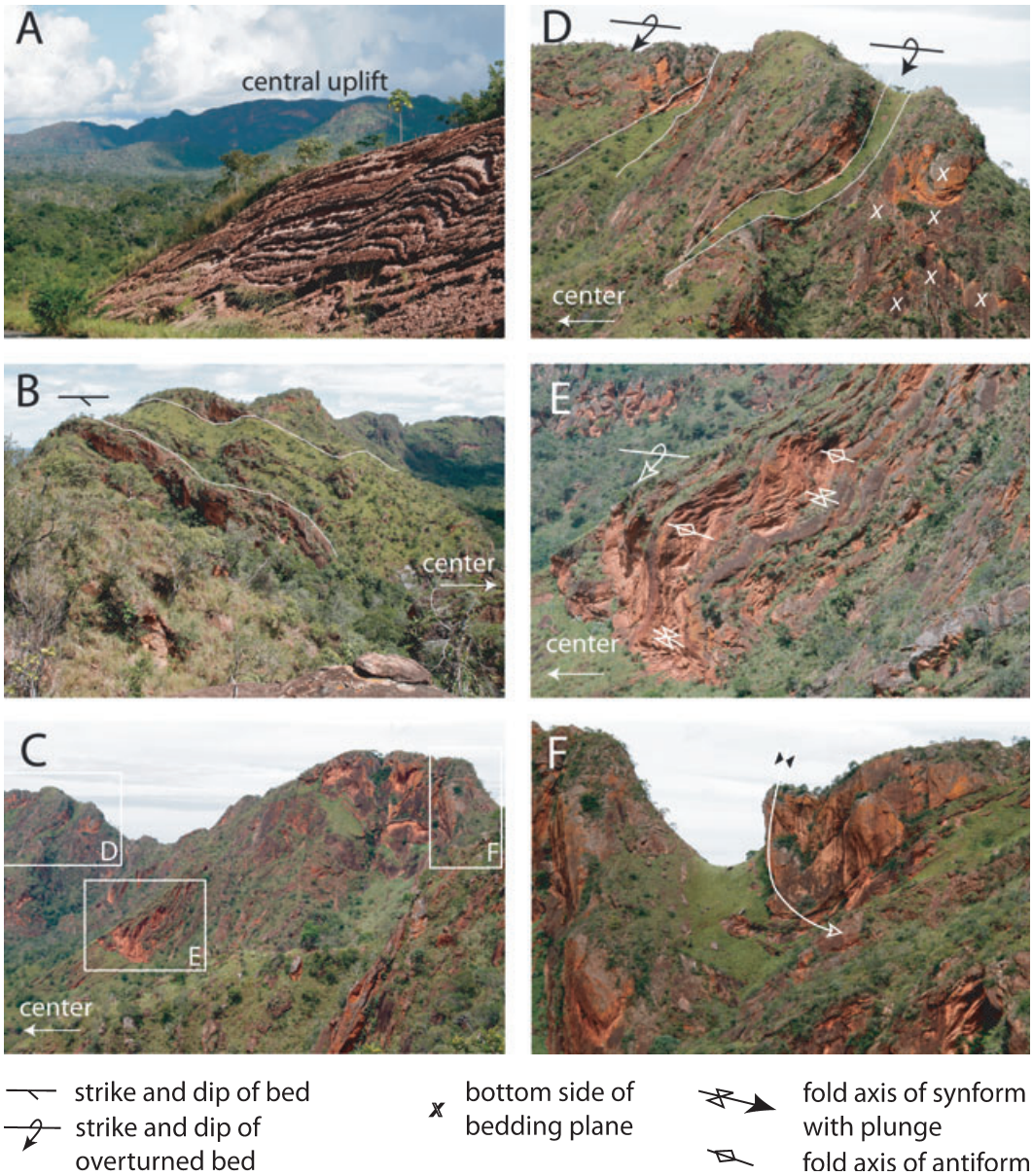

Fig. 4. Field photographs from the Serra da Cangalha impact structure. Locations of photographs are shown in Fig. 1. A) Gently inward (toward the crater center) dipping beds of Piauí Fm. sediments in the outer NW sector of the crater syncline. Strata are folded at the meter scale. The outward-directed vergency of the folds indicates top-outward motion that might be related to the excavation flow. Viewing direction is toward the central uplift (in SE direction). B) View along the southern crest of the collar of the central uplift toward the W. Note the oblique strike of the sandstone ridges with respect to the concentric trend of the collar. C) View along the northwestern and western collar toward the S. White rectangles indicate areas shown in photographs (D), (E), and (F): D) Strata of the Poti Fm. dipping toward the center of the structure and indicating overturning. E) Overturned beds of the Poti Fm. in the western collar of the central uplift. Beds show intense buckle folding at the meter scale. Fold axes and fold axial planes are horizontal (recumbent folds). F) Strata of the collar show prominent radial folding. The fold axis of the exposed fold plunges steeply toward the outside in its lower part and bends to an overturned orientation in its upper part.

the Poti Fm., its morphological resistivity is lower. However, the sandstone layers within Piauí Fm. are strong enough to form morphological ridges in the periphery of the central uplift.

The occurrence of chert marks the transition from the Piauí to the Pedra de Fogo Fm., which is part of the Permian Balsa Group and forms the uppermost stratigraphic unit exposed at Serra da Cangalha. These cherts are the result of silicification during diagenesis, and they are frequently and strongly brecciated. Due to their resistance to erosion, they form remarkable morphological ridges that define the outer perimeter of

the central uplift (Fig. 1). However, they are not continuous along the base of the Pedra de Fogo Fm. (Fig. 2). Silicified sandstones of the Pedra de Fogo Fm. form the flat tops of the table mountain land and mesas surrounding the Serra da Cangalha structure. As the strata of the Parnaíba basin are flat lying, an altitude of 400–420 m defines the transition between the Piauí and Pedra de Fogo formations. The area between the outer perimeter of the central uplift and the table mountains is only poorly and scarcely exposed, and mostly covered by soil and fluvial deposits. The occurrence of Pedra de Fogo Fm. in the crater moat could be verified only locally, e.g., by findings of Permian fossils such as *Psaronius Brasiliensis* (petrified wood) (Dias-Brito et al. 2007).

Crater Morphometry

On satellite imagery, in particular SRTM data, Landsat, and ASTER images, the Serra da Cangalha structure shows several discontinuous ring features. From the center to the rim, Reimold et al. (2006) distinguished (1) a central low-lying area of 2.2 km diameter, which they considered the collapsed central uplift of the structure, (2) a prominent inner circular structure with an outer perimeter of 3.2 km diameter, (3) a first intermediate circular feature with approximately 6 km diameter, (4) a second intermediate circular features at 11.0 km diameter, and (5) the crater rim with 12–13 km diameter (Fig. 1).

Field analysis showed that circular features are a topographic effect that reflects concentric exposures of lithologies with different resistance to erosion. The central depression corresponds to the exposure of Longá Fm. Reimold et al.'s (2006) inner circular structure is a prominent collar built up by massive silicified sandstones of the Poti Fm. The 200–370 m high collar is part of the central uplift of the structure, and is 2650–3075 m in diameter (mean Ø = 2830 m). The collar has a somewhat quadrangular, kite-like shape, and is open to the NNW (Adepelumi et al. 2004) (Figs. 1 and 2).

The first intermediate circular feature is formed by cliffs of steeply to vertically dipping brecciated chert and quartzites that form the lowermost unit of the Pedra de Fogo Fm. These concentric ridges are discontinuous, but stratiform. The formation of the ridges correlates with the degree of silicification of the strata and the formation of chert during diagenesis. The first intermediate circular feature delineates the central uplift at a diameter of 5300–6500 m (mean Ø = 5800 m).

The second intermediate circular feature of Reimold et al. (2006) is a subdued topographic elevation. It partly correlates with concentrically trending folds and monoclines within the ring syncline system, and some outcrops of chert breccias and silicified sandstones of the Pedra de Fogo Fm. The second intermediate circular feature roughly correlates with the perimeter of the occurrence of strata tilted due to impact crater collapse. The outer perimeter of the structure, interpreted as the crater rim affected by erosion, is topographically expressed by the termination of undeformed and flat lying table mountain and mesas. The abrupt termination of table mountains, in particular, in the southern part of the structure, indicates the presence of a concentric fault system. However, the throw is locally resolved as only a few meters. The current outer perimeter of the crater structure ranges from 13,000 to 14,000 m (mean Ø = 13,730 m). The structure has been widened slightly since impact time as the head scarp of the concentric normal fault has been eroded. In the northwestern sector of the crater, a concentrically trending monocline, whose inner limb dips toward the crater center, can be observed inside the crater rim (Fig. 4A). The region outside the crater is represented by a table mountain land dissected by fluvial drainage systems. The ratio of the diameters of the central uplift and the diameter of the outer rim fault is 0.42. McHone (1986) estimated a stratigraphic uplift of 740 m based on summation of stratigraphic thicknesses. This is in accordance with our analysis (Vasconcelos et al. 2010b). The application of the empirical relationship between the stratigraphic uplift SU and the crater diameter D for terrestrial craters, $SU = 0.006\ D^{1.1}$ (Grieve et al. 1981) would result in an uplift value of approximately 1000 m.

Lineament Analysis

Lineaments were mapped on CBERS-2B/HRC images inside and outside the crater to distances of more than 10 km from the crater center (Figs. 5 and 6A). Lineaments are interpreted as fracture planes and joints. These joints partly control the shape of escarpments and monadnocks in the crater rim zone and outside the crater, and influence the density of the vegetation cover. Our statistical analysis is based on more than 6200 digitized lineaments. Two prominent joint sets occur and strike at 102° (ESE–WNW) and 12° (NNE–SSW) both inside and outside the crater (Figs. 5 and 6). However, within the crater the scattering in orientation is larger and nearly all possible strike orientations occur. Joints of the 102° set are statistically the longest with lengths of up to 1000 m (Fig. 6B). There are no indications for concentric or radial lineament orientations within the crater.

The main joint sets at 102° and 12° appear to be unaffected by the presence of the crater, suggesting that they were formed after the impact or, if they were in existence prior to the impact, they were reactivated since the impact. These joints, thus, belong to a regional geological network of fissures of the Parnaíba basin and

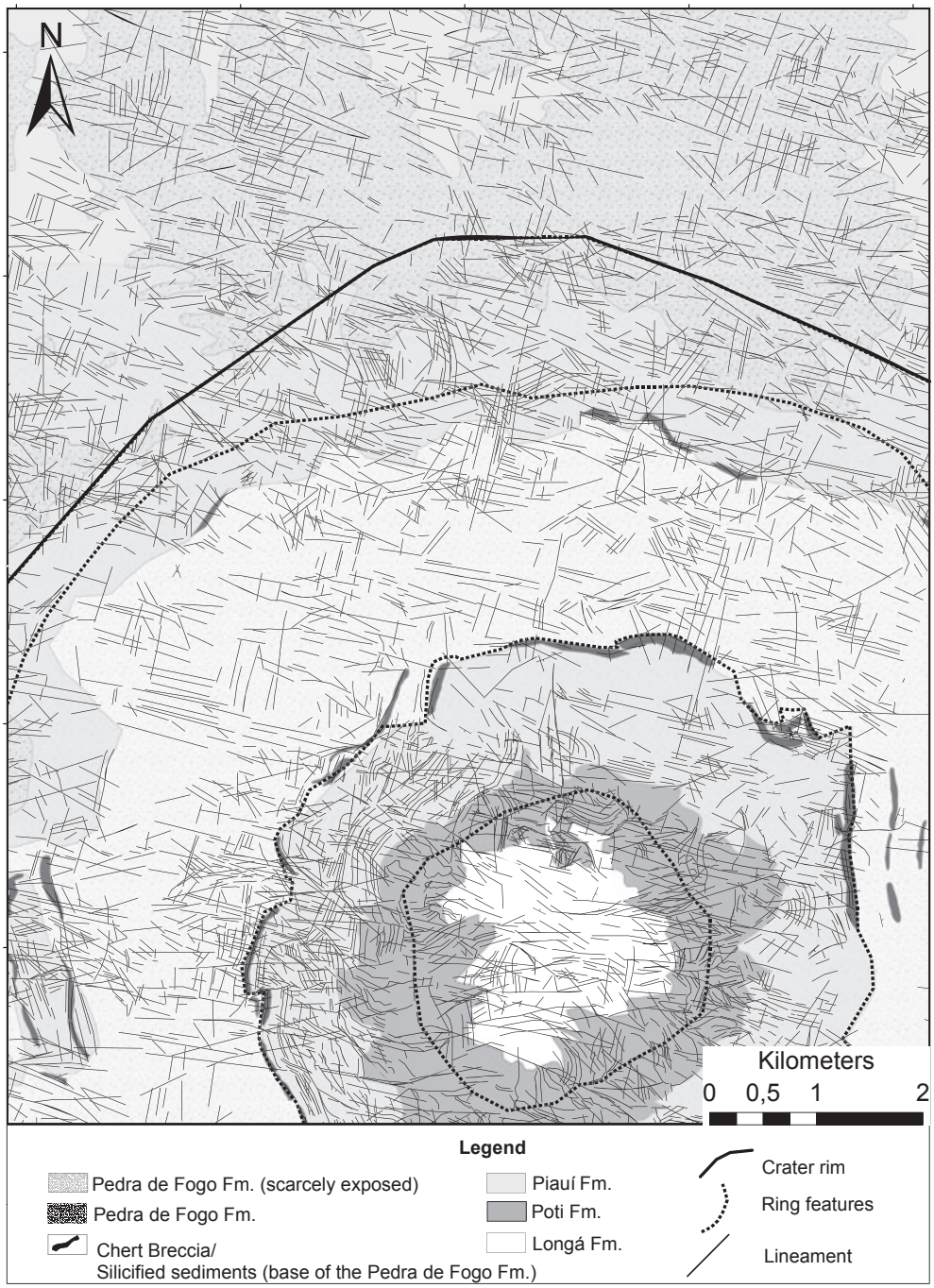

Fig. 5. Lineaments and fracture network of the northern and central part of the Serra da Cangalha impact structure as well as part of the region outside of the crater structure. Note that the two dominant sets of lineaments (NNE–SSW and ESE–WNW) occur both inside and outside the crater structure, thus postdating the impact event.

formed in a long-lasting and stable tectonic stress field. The NNE–SSW joint set is roughly coincident with the direction of the anomalous regional trend, which overlaps the magnetic data (Vasconcelos et al. 2010a). Impact-induced fracturing might be responsible for the large scattering of lineament strike orientations inside the crater structure. Almost all possible orientations are present, but the strike interval of 30–60° is seemingly under-represented.

Faults

Figures 2 and 7 show the mapped faults over the area of the entire crater and within the area of the

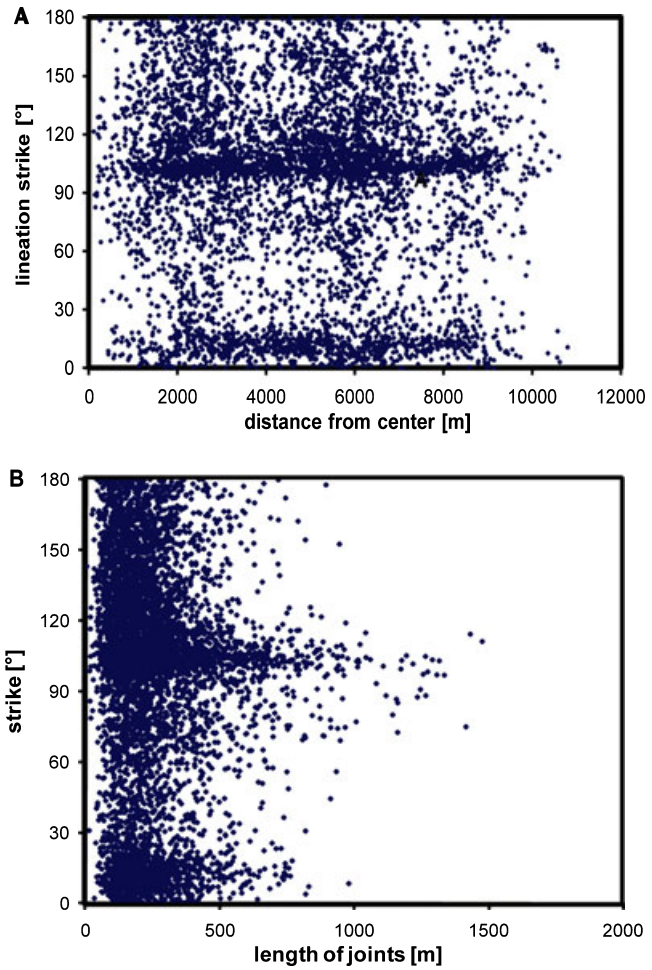

Fig. 6. A) Strike orientation of lineaments/joints as a function of their distance from the crater center. A distinct maximum of strike values occurs at 10° (NNE–SSW) and at 105° (WSW–ENE), for the entire radial variation. However, the variability in strike is particularly large at 2 and 6 km radial distance. B) WSW–ENE striking lineaments are among the longest and reach lengths of >1000 m.

central uplift, respectively. We mapped 435 faults with variable offsets and throws. The histogram in Fig. 8A shows that radial faults dominate over concentric ones (Fig. 8A). Figure 8B demonstrates that faults occur in every sector of the crater and show a wide variety of orientation with respect to the crater center. A concentration of faults with a strong radial component seems to occur in the ENE sector (60–90°) and in the SW sector (180–270°). Along these faults, blocks have been displaced stepwise forming domino-like stacks, as indicated in Fig. 3. The dominance of E–W (95°) striking faults correlates with the main lineament set and suggests that at least the ESE–WNW striking joint system must have been present prior to impact as planar zones of weakness. Joints were then activated as faults, where they have been in favorable orientation for slip. Major faults that correlate with the ESE–WNW striking regional joint system developed mainly in the southern part of the collar of the central uplift. They dissect the collar obliquely (Figs. 4B and 7). In the northern part of the central uplift some N–S striking faults developed that might be responsible for the erosive degradation of the collar in this sector of the crater.

Bedding and Folding

In the table mountain land outside the crater structure, beds are usually lying flat or show only a slight warping. Along the outer limb of the crater syncline, gentle dips toward the crater interior were found. Statistical analysis of all measured bedding planes shows that they dominantly strike concentrically (Fig. 9A), although the scatter is quite large. The standard deviation is ±38° of concentric deviation for all bedding data. The outer perimeter of the central uplift is marked by the sudden appearance of vertical beds of chert breccia (Fig. 7), which sometimes occur in en-echelon arrays and form narrow morphological ridges. The dip of strata within the collar changes with radial range, topographic altitude, and with the azimuthal position of the collar to the center. Although strata at the outer slope of the collar, near the transition from Poti Fm. to Piauí Fm., usually show steep, but normal dips, exposures along most parts of the inner slope near the transition to Longá Fm. display vertical or overturned beds. The same holds with elevation: overturned beds are particularly frequent at or near the crest of the collar. It is remarkable that almost all strata are overturned in the N, NW, and W sector of the inner collar (Fig. 3). The deviation from concentric strike and its statistical scattering increases with decreasing radial distance from the center. Although standard deviation of concentric strike is ±33° near the rim and along the moat (>4000 m distance from the center), the standard deviation increases to ±45° along the collar (<2000 m distance from the center). This means that virtually all strike directions occur.

The increased scattering in concentric deviation has two causes: Firstly, folds frequently occur in the collar (Fig. 7). Most fold axes plunge radially outward, so that strike orientation of beds in the limb produces a large variety of strike orientations (Fig. 4F). A rule of thumb in central uplifts is that the fold amplitude increases, whereas the fold wavelength decreases with decreasing radial distance. Thus, folds become increasingly tight until one of the limbs is sheared off. Radial fold formation is a spatial requirement during crater collapse and central uplift formation, as has been documented in a number of studies (Kriens et al. 1999; Kenkmann et al. 2005, 2010b; Kenkmann and Poelchau 2009). Secondly,

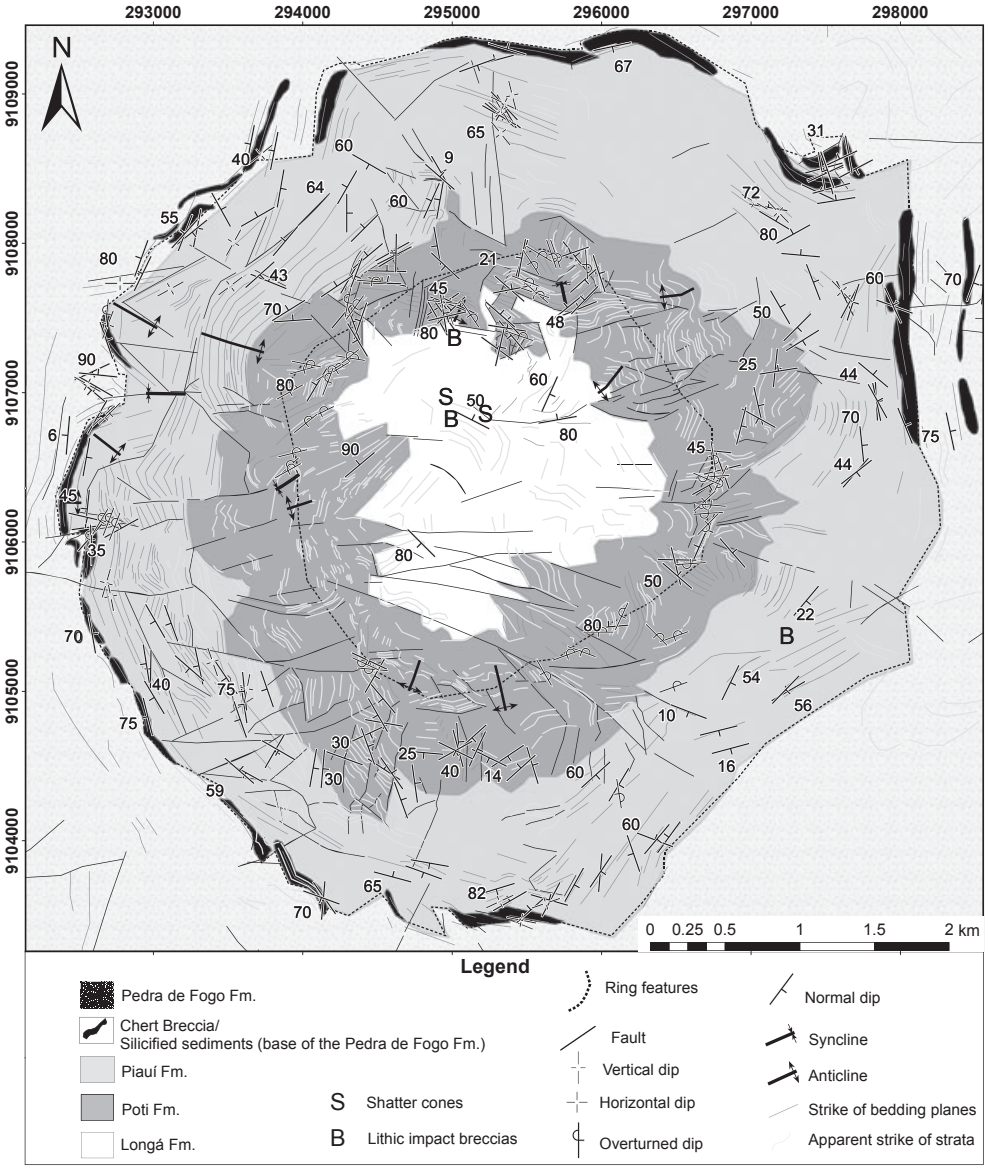

Fig. 7. Geological map of the central uplift of the Serra da Cangalha impact structure as revealed by field mapping supported by remote sensing analysis. The gross structure is that of a dome with the oldest rocks exposed in the center surrounded by successively younger strata. Brecciation of the Longá Fm. is too intensive to be mapped in detail. Strata mostly dip steeply or vertical. Overturning is most common in the northern half of the collar.

blocks bounded by faults show block rotation of variable degrees during translation, and this has caused strong deviations from concentric strike. Major slip planes for block translations are the preimpact, E–W striking joint sets (Fig. 4B) that were impact-activated especially in the southern part of the collar.

The overturned strata of the collar often show buckle folding at the meter scale to decameter scale (Fig. 4E). Buckle folding especially occurs in a layered rock sequence if a competence contrast between adjacent layers exists and flexural slip is possible. The observed buckle folds are recumbent folds and have horizontal or moderately dipping axial surfaces and subhorizontal fold hinges. Buckle folds may have been developed when the strata were tilted to a vertical position. If that is true, they document the loading caused by the weight of the central uplift. Buckle folding may thus indicate the onset of gravitational collapse of the central uplift under its own weight.

Microdeformation and Mesodeformation Structures

Macroscopic fracture surfaces have been described and were interpreted as shatter cones by McHone (1979).

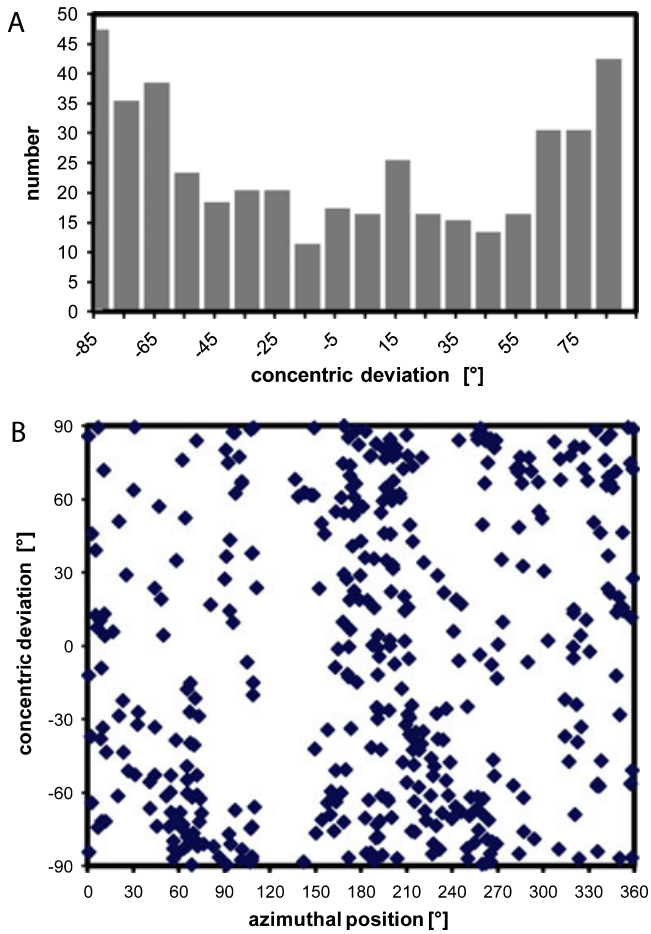

Fig. 8. Orientation of faults mapped in the central uplift. A) Histogram of the concentric deviation of faults with respect to the crater center. See text for details. The majority of faults strike radially. B) Azimuthal position of faults (with respect to the center of the impact structure) versus the concentric deviation of these faults. Faults in the central uplift are particularly frequent in the eastern sector (45–110° azimuthal position) and in the southwestern sector of the collar (165°–270°). The majority of these faults strike radially.

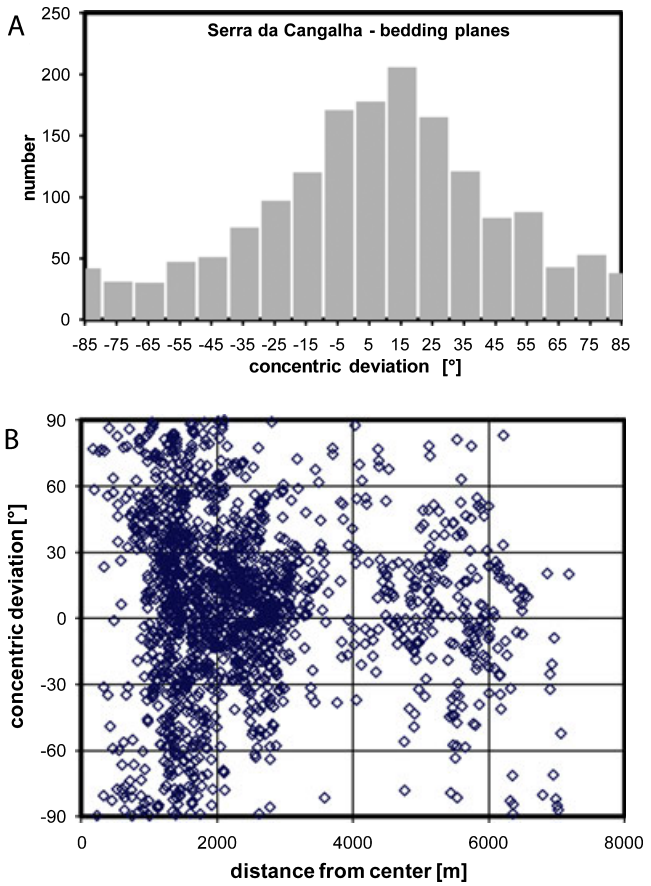

Fig. 9. Strike of bedding planes with respect to the crater center. A) The histogram indicates that concentrically striking beds are statistically the most frequent ones in the crater structure. However, the peak in the histogram is not exactly at 0° degree concentric deviation, but at 10–15°. B) Concentric deviation of strike versus distance from the crater center. Beds predominantly strike concentrically near the crater rim. In the periphery of the central uplift (2–3 km distance from the center, in Piauí Fm.) deviation from concentric strike varies from −60 to +60°. Along the collar (at approximately 1.5 km distance from the center, in Poti Fm) the entire range of strike orientations occurs.

We found rare samples of shatter cones of <1 decimeter size in coarse sandstone of the Longá Formation (Fig. 10A) on an isolated hill in the central crater depression inside the central uplift. The exact location is given in Figs. 7 and 10A. These shatter cones display a characteristic cone geometry with convergent grooves and ridges pointing to an apex (Fig. 10A). However, due to the coarse-grained character of the host lithology, the morphology of the surfaces is poorly resolved. The conical forms are built by numerous subcones (so-called horse-tailing). Cone angles are commonly 50–60°. Rare monomict and polymict breccias (Fig. 10B) were also found in the central depression and in the periphery of the central uplift. However, occurrence of polymict breccias as allochthonous infill of the crater moat could not be demonstrated. Brittle fracturing at the microscale, mesoscale, and macroscale is a ubiquitous feature of rocks exposed in the central uplift (Figs. 10C and 10D). Microbreccias from the borehole GT-01-GO (295860m E/9106341m N), situated in the innermost part of the central uplift, exhibit quartz grains with narrow-spaced straight lamellae, which are interpreted as basal planar deformation features (PDFs) (Fig. 11A). However, we did not find cross-cutting sets of lamellae. The thorough statistical analysis of possible PDFs and characterization of the amorphous state is beyond the scope of this article. Planar fractures (PFs) and so-called feather features (FFs) (French et al. 2004; Poelchau and Kenkmann 2011) (Figs. 11B and 11C) have been found in polymict breccias from the central depression and in

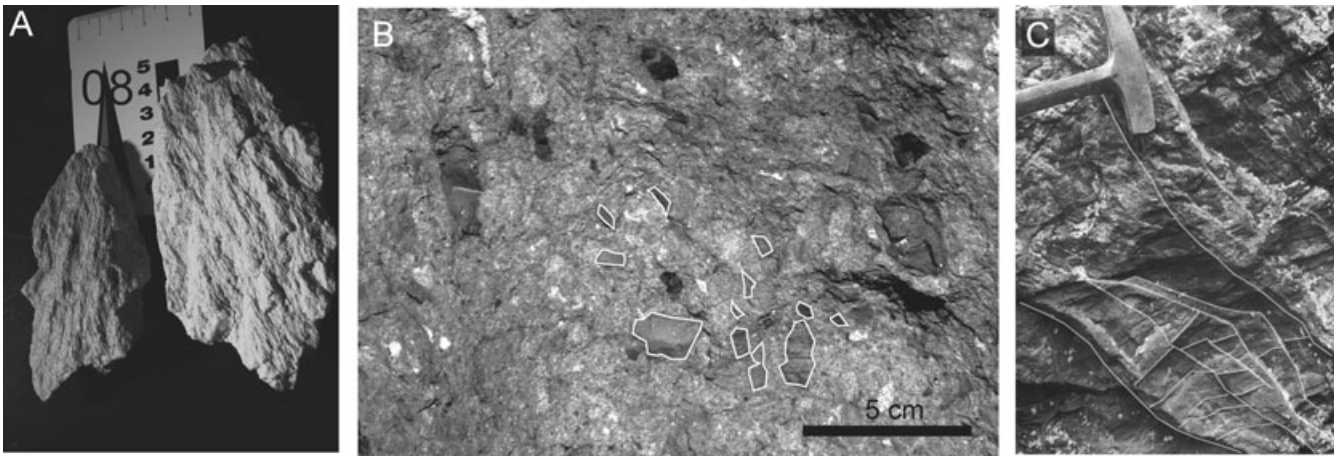

Fig. 10. A) Shatter cones formed in coarse-grained sandstone of the Longá Fm. in the central-northwestern sector of the central crater depression. Sample location: (295180m E/9106870m N). B) Polymict lithic breccia containing angular and subrounded quartz and claystone fragments embedded in a variegated matrix. Sample stems from the tectonized stratigraphic transition between Longá Fm. and Poti Fm. in the central-northwestern sector of the central crater depression. Sample location: (295,193 m E/9106894 m N). C) Stair-stepping and cross-cutting arrangement of small-scale fractures with millimeter to centimeter displacements in sandstone from the Poti Fm. Sample location: (295899 m E/9107743 m N).

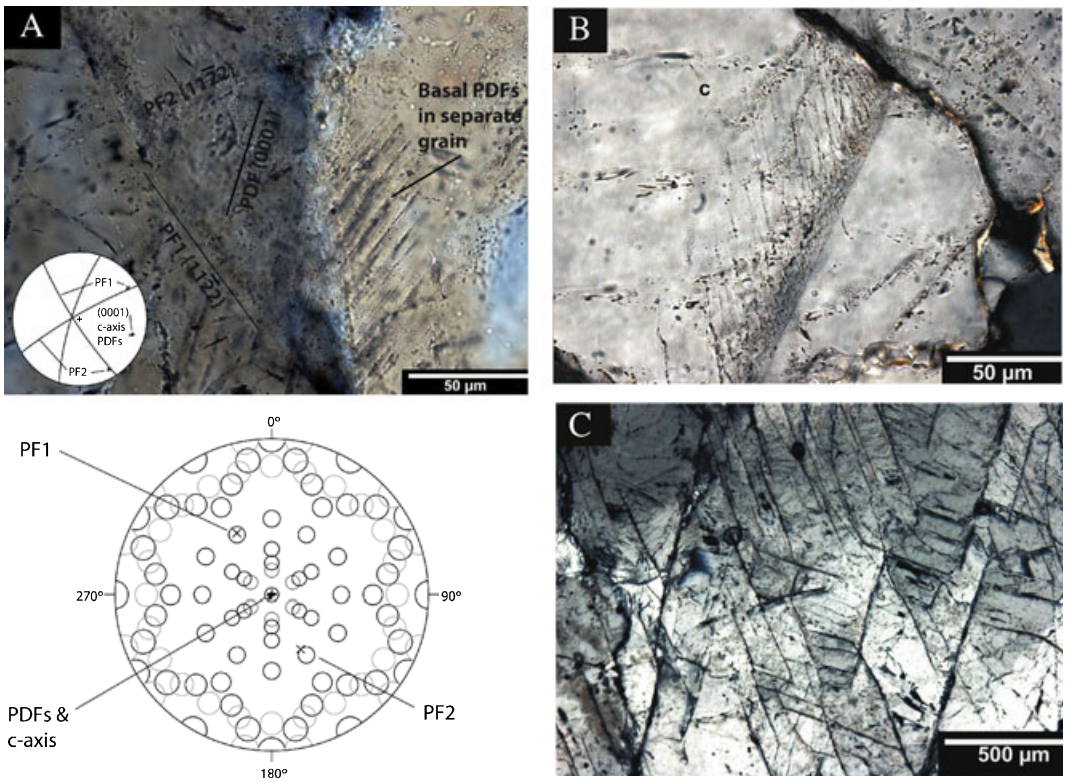

Fig. 11. A) Quartz with a single set of narrow-spaced (0001) planar deformation features (PDF) across a low angle grain boundary and a {11–22} planar fracture found in microbreccia from borehole GT-01-GO at approximately 90 m depth. Sample location: (295860 m E/9106341 m N) (viewed with crossed polarisers) (U-stage data by courtesy of Michael Poelchau, University of Freiburg). B) Feather features formed along the (0001) plane in quartz emanating from a planar fracture. Sample location: (295555 m E/9104510 m N). C) Abundant planar fractures (PF) in quartz grain from samples of polymict breccias found in the central crater depression. Sample location: (295180 m E/9106870 m N).

sandstones from the collar. FFs occur as short, parallel to subparallel lamellae, with spacings similar to that of PDFs. These lamellae are always found in combination with a PF. FFs are crystallographically controlled; (0001), {10–11}, {11–22} orientations are common, and {10–13} and {10–12} orientations are lacking. French et al. (2004) interpreted FFs as incipient PDFs. Poelchau and Kenkmann (2011) showed that their formation is linked to shearing along the associated PFs during the release from shock pressure in the low shock-pressure regime. The orientation of FFs in rock samples is suggested to be controlled by the direction of the principal axis of stress, with sheared PFs being oriented at approximately 45° angles to the axis and most FF lamellae aligned parallel to the axis.

DISCUSSION

Serra da Cangalha: Complex Impact Structure with a Central Uplift

The central uplift of this complex impact structure is compositionally heterogeneous with relatively incompetent beds in the center (Longá Fm.) surrounded by more competent massive sandstones (Poti Fm.). Ring-like features described by Reimold et al. (2006) are formed by selective erosion of the strata that have been uplifted to a central dome. Rocks are frequently overturned, in particular in the northern and western part. The central uplift shows signs of gravitational instability and collapse in the form of buckle folding of vertical and overturned strata (Fig. 4E), and overturning of beds in the upper part of the central uplift.

Effect of Impact Obliquity?

Recently, a number of field studies were carried out to elucidate the effect of an oblique impact onto the internal structure of the subsurface (e.g., Schultz and Anderson 1996; Scherler et al. 2006; Kenkmann and Poelchau 2009; Kenkmann et al. 2010b). Effects of impact obliquity on crater modification and the associated subsurface structure have long been neglected or even ruled out. One interesting exception is the paper by Boon and Albritton (1936) who suggested that an oblique impact should exhibit bilateral symmetry in the deep crater floor. Nonradial structural features indicative of an oblique projectile incidence are (1) dominance of a specific thrust direction within a central uplift (top down range), (2) bilateral symmetry and elongation of the central uplift, which may be divided into two parts, (3) occurrence of radial anticlines and synclines, preferentially parallel to the symmetry axis, (4) occurrence of normal dipping strata uprange and overturned strata downrange, and (5) normal plunging radial fold axes in uprange and overturned plunging fold axes in downrange direction. These deformation features suggest a downrange transport of rock and a central uplift that is initiated uprange and migrates downrange as the central uplift and crater grow to their final size. The validation of these features as diagnostic tools to infer the impact direction was possible at the elliptical impact structure Matt Wilson, Northern Territories, Australia (Kenkmann and Poelchau 2009), as well as for Martin crater on Mars, where an asymmetric ejecta blanket provided independent proof of the impact trajectory (Poelchau et al. 2009). These findings are in agreement with flow fields inferred from numerical models of oblique impact cratering (Shuvalov and Dypvik 2004; Elbeshausen et al. 2007).

The central uplift of Serra da Cangalha (Fig. 7) shows some asymmetries that match the presented criteria and could be indicative for an oblique impact. These are (1) the quadrangular, kite-like shape of the collar with a symmetry plane NNE/SSW, (2) an elongation of the central uplift's collar along the NNE/SSW diagonal, (3) the preferred overturning of strata in the northern to western sectors (Fig. 3), and (4) the dominance of E–W striking (faults crossing the collar obliquely and delineating equally oriented blocks).

Features (1), (2), and (4) may be interpreted in terms of an impact either from the NNE or from the SSW. Feature (3) defines a trajectory that is oriented more NNW–SSE and makes an impact from the SSE more likely. From experience with other oblique impact structures such as Upheaval Dome, Matt Wilson, Spider, Gosses Bluff, and Waqf as Suwwan, features (3) and (4) have the greatest significance for reconstructing the impact direction. However, the dominance of E–W striking faults at Serra da Canghalha as an argument for an impact trajectory perpendicular to strike is arguable as this correlates with the preimpact joint system. We conclude that signatures for an oblique impact are present at Serra da Cangalha, though not pronounced and also overprinted by effects related to target heterogeneity (see the Effect of Target Heterogeneities? section). Collectively, however, they suggest an impact from a southerly direction of unknown incidence.

Effect of Target Heterogeneities?

Heterogeneous targets influence style and degree of crater excavation and collapse and, thereby, the final geometry of impact structures (Eppler et al. 1983; Öhman 2009 and references therein; Öhman et al. 2010). The contrast in strength of the rocks involved in the cratering process and the spatial arrangement of zones of weakness determine how intensely such heterogeneities

affect the stress and strain distribution, and the resulting cratering flow field in the target. For instance, the vertical arrangement of a pre-existing rectangular joint and fissure pattern at Barringer crater (Meteor Crater), Arizona, USA, resulted in a more efficient excavation flow along the fissures (Eppler et al. 1983; Poelchau et al. 2009) than between them. In polygonal complex impact structures, crater modification obliterates the excavation flow and the straight segments are mostly parallel to the zones of weakness (Eppler et al. 1983).

The presence of a horizontal layering with alternating competent and incompetent beds, which is typical for sedimentary basins, also causes a substantial strength anisotropy. The critical resolved shear stress for bedding-parallel movements is much less intense than for movements perpendicular to the layers. This can result in the formation of low-angle faults and detachments during crater collapse, whereby strain is localized into the weaker beds. Collins et al. (2008) have shown that a horizontal layering of the target can affect the intensity of crater collapse, and also expands the zone of collapse.

The Serra da Cangalha impact structure shows both types of heterogeneities (1) a horizontal rheological stratification with interlayered competent (sandstones) and incompetent (shale) sediments, and (2) a prominent orthogonal system of vertical joints trending NNE–SSW and WNW–ESE. Despite some irregularities, the outer crater perimeter shows straight segments on the north, west, and south sides, which run parallel to the mapped joint sets (compare Figs. 1, 2, and 5). This is in accordance with polygonal complex craters (Eppler et al. 1983; Öhman et al. 2010). Joints near the crater rim were most likely reactivated as normal faults and then accommodated downfaulting of slump blocks into the crater cavity during crater modification. Thus, crater rim faults adopted the orientation and the straight extent of the joints.

The central uplift also has an angular character and a shape resembling a deltoid or kite (a quadrilateral with two disjoint pairs of congruent adjacent sides), at least when tracing the crest line of the collar. The diagonals of the kite run roughly parallel to the main preimpact joint sets. The rectangular joint system and the bedding planes were rotated during the formation of the central uplift. If we assume, for the sake of simplicity, a rotation by 90° throughout the central uplift in such a way that bedding planes were rotated into a vertical position (which is a reasonable approximation), the passive rotation of the joints would have led to the following constellation. (1) In the WNW, NNE, ESE, and SSW sectors of the central uplift one set of joints remained in vertical position in each case and was unaffected in orientation, whereas the other set was moved into a horizontal position. (2) In all other sectors, both joint sets changed

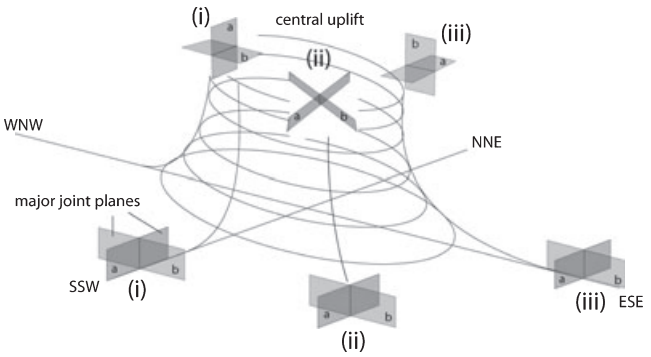

Fig. 12. Pre-existing joint sets along NNE–SSW (plane "a") and WNW–ESE (plane "b") are rotated during central uplift formation. The orientation of a planes "a" and "b" remains unaffected during tilting only, if the planes strike radially with respect to the impact center, e.g., plane "a" in (i) or plane "b" in (iii) they keep their orientation (strike and dip is constant before and after the rotation) during rotation, whereas in (ii) planes "a" and "b", they change their orientation. Thus, in the ESE and WNW sector of the crater, the WNW–ESE striking joints did not change their orientation during central uplift formation, whereas in the SSW and NNE sector of the crater, the NNE–SSW striking joints remain unchanged.

their orientation during rotation and assumed final dips of variable attitude (Fig. 12). More specifically, ESE–WNW striking joints kept their orientation in the WNW and ESE sectors during central uplift formation, whereas SSW–NNE striking joints kept their orientation in the NNE and in the SW sectors.

In this simplified model, all strata would dip vertically and strike concentrically. This is in contrast to our mapping results that show partly strong concentric deviations of strata in the central uplift. We assume that those joints that did not change their dip and strike during central uplift formation, largely controlled the deformation, and possibly induced a block-wise rotation of strata. The quadrangular shape of the collar of the central uplift is not caused by beds that strike parallel to straight segments. The latter is known from the central uplifts of the Vredefort Dome, South Africa (Antoine et al. 1990; Wieland et al. 2005), or the Araguainha structure, Brazil (Lana et al. 2007). The most prominent features in these crater structures are kilometer-long straight ridges that are separated by radial fault zones. The angular shape of the central uplift of the Serra da Cangalha impact crater is rather a product of the block-wise disintegration of the target.

CONCLUSIONS

Main results of this geological and structural survey of the entire Serra da Cangalha structure are:

1. New shatter cone findings and the occurrences of PFs, FFs, and possible PDFs along with the

structural data support the impact origin of Serra da Cangalha.

2. Serra da Cangalha is a complex impact structure formed in flat lying Devonian to Permian sedimentary rocks and has a current crater diameter of 13,700 m and a central uplift diameter of 5800 m. A lower limit for the stratigraphic uplift is 700 m. Circular features observed in remote-sensing imagery are due to selective erosion of circumferentially striking beds of quartzitic sandstones and shales in the center of the crater. There are no indications that the morphological depression in the center of the central uplift is comparable to a central pit that is typical for many Martian impact craters (Barlow 2006). We roughly estimate approximately 500 m of erosion since the time of impact. This estimate is based on the preserved shock features in the central uplift that suggest peak shock pressures of not more than 10 GPa, and the apparent lack of allochthonous breccias fill in the crater moat. If the estimate of erosion is correct, the original crater diameter would have been 14–14.5 km.
3. NNE–SSW and WNW–ESE striking joint sets were present prior to the impact. This tectonic strain field also overprinted the structure after its formation. As preferred zones of weakness, the preimpact joints partly controlled the geometry of the outer polygonal perimeter of the structure and, in particular, the deformation within the central uplift. Joints in radial orientation to the impact center did not undergo a change in orientation upon strata tilting during central uplift formation (e.g., E–W striking joints in the eastern or western sector of the central uplift). These planes played a dominant role during central uplift formation.
4. The asymmetry of the central uplift with a preferred overturning of strata in the northern to western sector may suggest a moderately oblique impact from a southerly direction, although the structural signal is not strong and obliterated by effects caused by target heterogeneity.
5. Buckle folding of tilted strata, as well as strata overturning indicates that the central uplift became gravitationally unstable at the end of crater formation.

Acknowledgments—W. U. R. and T. K. acknowledge travel support from the German Research Foundation (DFG), through the Re 528/9–1 and/11–1 grants (to W. U. R.). A. P. C. and M. A. R. V. were supported by the State of São Paulo Research Foundation (FAPESP), through grant 2008/53588–7, and also acknowledge the Brazilian National Council for Scientific and Technological Development (CNPq) for research grant 30334/2009–0 (A. P. C.) and Ph.D. grant (M. A. R. V.). M. A. R. V. is also grateful for a grant by the German Academic Exchange Service (DAAD) that allowed him to collaborate closely with the German team in Berlin and Freiburg throughout 2010. DigitalGlobe is acknowledged for providing WorldView-1 satellite data and M. Poelchau for assisting with U-stage measurements. We are very grateful to T. Öhman, G. S. Collins, and the associate editor A. Deutsch for very thorough and constructive reviews.

Editorial Handling—Dr. Alexander Deutsch

REFERENCES

Abraham A. A., Flexor J. M., and Fontes S. L. 2004. Geophysical signature of Serra da Cangalha impact crater, Brazil (abstract). *Meteoritics & Planetary Science* 39:A11.

Adepelumi A. A., Fontes S. L., and Flexor J. M. 2004. Environmental perturbations caused by the Serra da Cangalha impact crater structure, northeastern Brazil. *Environtropica* 1:58–71.

Adepelumi A. A., Fontes S. L., Schnegg P. A., and Flexor J. M. 2005a. An integrated magnetotelluric and aeromagnetic investigation of the Serra da Cangalha impact crater, Brazil. *Physics of the Earth and Planetary Interiors* 150:159–181.

Adepelumi A. A., Flexor J. M., and Fontes S. L. 2005b. An appraisal of the Serra da Cangalha impact structure using the Euler deconvolution method. *Meteoritics & Planetary Science* 40:1149–1157.

Almeida-Filho R., Moreira F. R. S., and Beisl C. H. 2005. The Serra da Cangalha astrobleme as revealed by ASTER and SRTM orbital data. *International Journal of Remote Sensing* 26:833–838.

Antoine L. A. G., Nicolaysen L. O., and Nicol S. L. 1990. Processed and enhanced gravity and magnetic images over the Vredefort structure and their interpretation. *Tectonophysics* 171:63–74.

Barlow N. G. 2006. Impact craters in the northern hemisphere of Mars: Layered ejecta and central pit characteristics. *Meteoritics & Planetary Science* 41:1425–1436.

Boon J. D. and Albritton C. C. 1936. Meteorite craters and their possible relationship to "cryptovolcanic structures." *Field and Laboratory* 5:1–9.

Collins G. S., Morgan J., Barton P., Christeson G. L., Gulick S., Urrutia J., Warner M., and Wünnemann K. 2008. Dynamic modeling suggests terrace zone asymmetry in the Chicxulub crater is caused by target heterogeneity. *Earth and Planetary Science Letters* 270:221–230.

Crósta A. P. 1982. Estruturas de impacto no Brasil: uma síntese do conhecimento atual. *Anais do XXXII Congresso Brasileiro de Geologia*, Salvador, Bahia, vol. 4:1372–1377.

Crósta A. P. 1987. Impact structures in Brazil. In *Research in terrestrial impact structures*, edited by Pohl J. Wiesbaden: Vieweg and Sons. pp. 30–38.

Crósta A. P. 2004. Impact craters in Brazil: How far we've gotten. *Meteoritics & Planetary Science* 39:A27.

Dias-Brito D., Rohn R., Castro J. C., Dias R. R., and Rössler R. 2007. The Northern Tocantins Petrified Forest, State of Tocantins—The most luxuriant and important Permian tropical-subtropical floristic record in the southern hemisphere. In *Geological and palaeontological sites of*

Brazil, edited by Winge M., Schobbenhaus C., Berbert-Born M., Queiroz E. T., Campos D. A., Souza C. R. G., and Fernandes A. C. S. Brasília: DNPM/CPRM—Comissão Brasileira de Sítios Geológicos e Paleobiológicos (SIGEP). 554 p.

Dietz R. S. and French B. M. 1973. Two possible astroblemes in Brazil. *Nature* 244:561–562.

Elbeshausen D., Wünnemann K., and Collins G. S. 2007. Three-dimensional numerical modeling of oblique impact processes: Scaling of cratering efficiency (abstract #1952). 38th Lunar and Planetary Science Conference. CD-ROM.

Eppler D. T., Ehrlich R., Nummedal D., and Schultz P. H. 1983. Sources of shape variation in lunar impact craters. Fourier shape analysis. *Geological Society of America Bulletin* 94:274–291.

French B. M., Cordua W. C., and Plescia J. B. 2004. The Rock Elm meteorite impact structure, Wisconsin: Geology and shock-metamorphic effects in quartz. *Geological Society of America Bulletin* 116:200–218.

Góes A. M. O. and Feijó F. J. 1994. Bacia do Parnaíba. *Boletim de Geociéncias da Petrobrás* 8:57–67. In Portugese.

Grieve R A. F., Robertson P. B., and Dence M. R. 1981. Constraints on the formation of ring impact structures, based on terrestrial data. In *Multi-ring basins: Formation and evolution*, edited by Schultz P. H. and Merrill R. B. Proceedings, 12th Lunar and Planetary Science Conference, New York: Pergamon. pp. 37–57.

Kenkmann T. and Poelchau M. H. 2009. Low-angle collision with Earth: The elliptical impact crater Matt Wilson, NT, Australia. *Geology* 37:459–462.

Kenkmann T., Jahn A., Scherler D., and Ivanov B. A. 2005. Structure and formation of a central uplift: A case study at the Upheaval Dome impact crater, Utah. In *Large meteorite impacts III* edited by Kenkmann T., Hörz F. and Deutsch A. GSA Special Paper 384. Boulder, Colorado: Geological Society of America. pp. 85–115.

Kenkmann T., Vasconcelos M. A. R., Crosta A. P., and Reimold W. U. 2010a. Serra da Cangalha, Tocantins, Brazil: Insights into the structure of a complex impact crater with an overturned central uplift (abstract #1237). 41st Lunar and Planetary Science Conference. CD-ROM.

Kenkmann T., Reimold W. U., Khirfan M., Salameh E., Khoury H., and Konsul K. 2010b. The complex impact crater Jebel Waqf as Suwwan in Jordan: Effects of target heterogeneity and impact obliquity on central uplift formation. In *Large meteorite impacts and planetary evolution IV*, edited by Gibson R. L. and Reimold W. U. GSA Special Paper 465. Boulder, Colorado: Geological Society of America. pp. 471–487.

Kriens B. J., Shoemaker E. M., and Herkenhoff K. E. 1999. Geology of the Upheaval Dome impact structure, southeast Utah. *Journal of Geophysical Research* 104: 18,867–18,887.

Lana C., Souza Filho C. R., Marangoni Y. R., Yokoyama E., Trindade R. I. F., Tohver E., and Reimold W. U. 2007. Insights into the morphology, geometry, and post-impact erosion of the Araguainha peak-ring structure, central Brazil. *Geological Society of America Bulletin* 119:1135–1150.

McHone J. F. 1979. Riachao Ring, Brazil; a possible meteorite crater discovered by the Apollo astronauts. In *Apollo-Soyuz test project summary science report*, vol. II, edited by El-Baz F. and Warner D. M. Earth observations and photography. NASA Special Publication No. SP-412, pp. 193–202.

McHone J. F. 1986. Terrestrial impact structures: Their detection and verification with two new examples from Brasil. Ph.D. thesis. University of Illinois at Urbana-Champaign, Urbana, Illinois, USA.

Öhman T. 2009. The structural control of polygonal impact craters. Ph.D. thesis. Publications of the Department of Geosciences, University of Oulu, Oulu, Finland.

Öhman T., Aittola M., Korteniemi J., Kostama V.-P., and Raitala J. 2010. Polygonal impact craters in the solar system: Observations and implications. In *Large meteorite impacts and planetary evolution IV*, edited by Gibson R. L. and Reimold W. U. GSA Special Paper 465. Boulder, Colorado: Geological Society of America. pp. 51–65.

Poelchau M. H. and Kenkmann T. 2008. Asymmetric signatures in simple craters as an indicator for an oblique impact vector. *Meteoritics & Planetary Science* 43:2059–2072.

Poelchau M. H. and Kenkmann T. 2011. Feather features: A low shock pressure indicator in quartz. *Journal of Geophysical Research* 116: B02201, doi:10.1029/2010JB007803.

Poelchau M. H., Kurta A. T., and Kenkmann T. 2009. Signatures of an oblique impact in the central uplift of Martin crater, Mars (abstract #1796). 40th Lunar and Planetary Science Conference. CD-ROM.

Reimold W. U., Cooper G. R. J., Romano R., Cowan D. R., and Koeberl C. 2006. Investigation of Shuttle Radar Topography Mission (SRTM) data of the possible impact structure at Serra da Cangalha, Brazil. *Meteoritics & Planetary Science* 41:237–246.

Santos U. P. and McHone J. F. 1979. Field report on Serra da Cangalha and Riachão circular features. *Instituto de Pesquisas Espacias (INPE)* Rel. 1458-NTE/153: 13.

Scherler D., Kenkmann T., and Jahn A. 2006. Structural record of an oblique impact. *Earth and Planetary Science Letters* 248:28–38.

Schultz P. H. and Anderson R. R. 1996. Asymmetry of the Manson impact structure: Evidence for impact angle and direction. In *The Manson impact structure, Iowa: Anatomy of an impact crater*, edited by Koeberl C. and Anderson R. R. GSA Special Paper 302. Boulder, Colorado: Geological Society of America. pp. 397–417.

Shuvalov V. V. and Dypvik H. 2004. Ejecta formation and crater development of the Mjølnir impact. *Meteoritics & Planetary Science* 39:467–479.

Vasconcelos M. A. R., Crósta A. P., and Molina E. C. 2010a. Geophysical characteristics of four possible impact structures in the Paraíba basin, Brazil: Comparison and implications. In *Large meteorite impacts and planetary evolution IV*, edited by Gibson R. L. and Reimold W. U. GSA Special Paper 465. Boulder Colorado: Geological Society of America. pp. 201–217.

Vasconcelos M. A. R., Góes A. M., Crósta A. P., Kenkmann T., and Reimold W. U. 2010b. Serra da Cangalha impact structure, Parnaíba basin, northeastern Brazil: Target characterization and stratigraphic estimates of the uplift (abstract #1868). 41st Lunar and Planetary Science Conference. CD-ROM.

Wieland F., Gibson R. L., and Reimold W. U. 2005. Structural analysis of the collar of the Vredefort Dome, South Africa—Significance for impact-related deformation and central uplift formation. *Meteoritics & Planetary Science* 40:1537–1554.